DNA-Based Biosensor for Monitoring pH *in Vitro* and in Living Cells†

Tatsuo Ohmichi,‡,§ Yasunori Kawamoto,|| Peng Wu,⊥ Daisuke Miyoshi,‡ Hisae Karimata,|| and Naoki Sugimoto*,‡,||

Frontier Institute for Biomolecular Engineering Research (FIBER), Konan University, 8-9-1 Okamoto, Higashinada-ku, Kobe 658-8501, Japan, I.S.T. Corporation, 13-13-5 Ichiriyama, Otsu 520-2153, Japan, Department of Chemistry, Faculty of Science and Engineering, Konan University, 8-9-1 Okamoto, Higashinada-ku, Kobe 658-8501, Japan, and High Technology Research Center, Konan University, 8-9-1 Okamoto, Higashinada-ku, Kobe 658-8501, Japan

Received October 31, 2004; Revised Manuscript Received January 18, 2005

ABSTRACT: DNA is a promising material for the construction of a biosensor or bioindicator because its structure is sensitive to the binding of cofactors. In the current studies, we found that a combination of two DNA oligonucleotides, 5′-TCTTTCTCTTCT-3′ and 5′-AGAAAGAGAAGA-3′, exhibit a novel structural transition from a Watson−Crick antiparallel duplex to a parallel Hoogsteen duplex as the pH changes from pH 7.0 to 5.0. By labeling this DNA for fluorescence resonance energy transfer, we were able to develop a sensitive pH indicator that can detect changes between pH 7.0 and 5.0. Moreover, using DNA-based hairpin parallel-stranded duplex in conjunction with fluorescence microscopy, we were able to observe the pH changes in living cells during apoptosis as an easily detected change in color. These results indicate that the DNA-based pH indicator should be useful for detecting pH changes between pH 7.0 and 5.0 in living cells.

Understanding changes in various intracellular conditions, including cation concentrations and pH, can help elucidate physiological and pathogenic processes. Characterization of these intracellular changes depends on the development of suitable biological sensors. Nucleotide-based indicators or sensors are very promising in this regard because their conformations are very sensitive to interaction with other molecules or ions. Indeed, several studies indicate that DNA- or RNA-based aptamers or ribozymes can be used to create intelligent sensors with high specificity for target molecules (*1*−*3*). A major advantage of nucleotide-based sensors is that the highly ordered structure formed by DNA or RNA can be thermodynamically controlled and, thus, improved by rational design (*4*−*9*). Indeed, in our previous studies, we used rational design to control the thermodynamics of deoxyribozyme, which was placed on a surface plasmon resonance (SPR) sensor chip to detect RNA folding (*10*, *11*).

Changes in pH are important for a variety of cellular processes. For example, in neutrophils, stimulus-induced alkalinization is thought to modulate chemotaxis, phagocytosis, and secretion of superoxide radicals (*12*, *13*). Moreover, intracellular alkalinization is an early event in the stimulation of mitogenesis in mammalian fibroblasts, wherein it may be necessary for the initiation of DNA synthesis (*14*, *15*). Low pH also leads to various events such as hyperuricemia, gout, and apoptosis (*16*). Measurements of pH in humans also indicate a difference between tumor and normal tissues. For measurement of intracellular pH, BCECF (2′,7′-bis-(2-carboxyethyl)-5-(and 6)-carboxyfluorescein) and GFP (green fluorescent protein) are commonly used (*17*−*19*). These indicators, however, show only a single color that does not change substantially with the pH. Thus, more effective methods for monitoring the intracellular pH are needed.

Here, we describe studies on the use of a DNA-based indicator for monitoring intracellular pH. This indicator takes advantage of a novel structural transition in a DNA duplex that occurs when the pH changes. We began by investigating the structural transition of a parallel Hoogsteen duplex, which is designed to form a stable duplex at low pH upon protonation of a C base. Thereafter, we combined the parallel Hoogsteen duplex with labels for fluorescence resonance energy transfer (FRET), generating a probe that changes in color according to the pH and that can be used both *in vitro* and in living cells. These results show that DNA is a good material for developing improved pH probes that can be used in living cells.

MATERIALS AND METHODS

Oligonucleotide Synthesis. The 12-mer DNA oligonucleotides, 5′-TCTTTCTCTTCT-3′ (PyH1) and 5′-AGAAAGAGAAGA-3′ (PuC1), and the 24-mer 5′-TCTTTCTCTTCT-3′/3′-TTTTAGAAGAGAAAGA-5′ were synthesized on a solid support using the standard phosphoramidite chemistry process on an Applied Biosystems model 391 DNA synthesizer. These oligonucleotides were purified by HPLC with Wakosil-II 5C18RS cartridges after deblocking operations as described previously (*12*). The oligonucleotides were further purified and desalted with Sep-Pak C-18 cartridges. The final purity of the oligonucleotides was confirmed by HPLC. For circular dichroism (CD),[1] ultraviolet spectroscopy

† This work was supported in part by Grants-in-Aid for Scientific Research and "Academic Frontier" Project (2004−2009) from MEXT, Japan.

* To whom correspondence should be addressed. E-mail: sugimoto@konan-u.ac.jp. Telephone: +81-78-435-2497. Fax: +81-78-435-2539.

‡ Frontier Institute for Biomolecular Engineering Research (FIBER), Konan University.

§ I.S.T. Corporation.

|| Department of Chemistry, Faculty of Science and Engineering, Konan University.

⊥ High Technology Research Center, Konan University.

10.1021/bi0476782 CCC: $30.25
Published on Web 04/20/2005

(UV) melting, and FRET measurements, the oligonucleotides were mixed with 100 mM Na^+ and one of the following buffers: 50 mM Tris-acetate at pH 5.0, 50 mM MES at pH 6.0 or 7.0, or 50 mM Tris-HCl at pH 8.0 or 9.0. Single-strand concentrations were determined by measuring the absorbance (260 nm) at 85 °C. The different DNA strands were mixed in equimolar amounts, and the total species concentrations were estimated by averaging the extinction coefficients of the single strands (*12*).

CD Measurements. CD spectra were recorded on a Jasco J-820 spectropolarimeter equipped with a PTC-423L temperature controller. For each sample, at least 4 spectrum scans were accumulated over a wavelength range from 190 to 350 nm and a temperature of 1.0 °C in 0.1 cm path-length cell at a scanning rate of 10 nm/min. The scan of the buffer alone was subtracted from the average scan for each sample. CD spectra were collected in units of millidegrees, normalized to the total species concentrations, and then converted to θ. The cell-holding chamber was flushed with a constant stream of dry nitrogen to avoid water condensation on the cell exterior. All measurements were conducted at a total species concentration of 70 μM.

UV Melting Measurements. Absorbance measurements in the UV region were made on Shimadzu UV-1700 spectrophotometers. Melting curves (absorbance versus temperature curves) were measured at 260 nm with these spectrophotometers connected to a Shimadzu TMSPC-8 thermoprogrammer. A heating rate of 0.5 °C/min was used for all measurements. Water condensation on the cuvette exterior at the low-temperature range was avoided by flushing with a constant stream of dry N_2 gas. Prior to the experiment, the buffer was degassed with an ultrasonic wave for 5 min. As described elsewhere (*13*), all melting curves were determined with a curve-fitting procedure to obtain the enthalpy ($\Delta H°$), entropy ($\Delta S°$), and free-energy changes at 37 °C ($\Delta G°_{37}$) for the formation of the nucleic acid duplex.

FRET Measurements. In the FRET experiment, fluorescein isothiocyanate (FITC) was used as the donor and tetramethylrhodamine (TAMRA) was used as the acceptor. FITC and TAMRA were coupled to the 5′ termini as phosphoramidites. All measurements were carried out with excitation at 494 nm, the excitation wavelength of FITC. FRET assays were performed at 1 °C using 4 μM PyH1 and PuC1.

Fluorescence Microscopy. MCF-7 cells (approximately 1×10^5) were seeded in culture flasks for 1 day with and without 100 nM [D-Trp^8]SST for fluorescence microscopy experiments. Cultures were incubated at 37 °C and 5% CO_2 in Dulbecco's Modified Eagle's medium (DMEM) containing 10% fetal bovine serum (FBS) and antibiotics (penicillin and streptomycin). The medium was removed from the cultures, and the cells were washed 3 times with phosphate-buffered saline (PBS). The pH sensor was prepared for transfection by equilibrating 90 μL of 6 μM pH sensor in DMEM without 10% FBS and antibiotics. Next, 3 μL of LipofectAMINE 2000 reagent (Invitrogen) was activated in 10 μL of DMEM without 10% FBS and antibiotics by equilibration for 10 min at room temperature. The pH sensor mixture and activated LipofectAMINE were mixed together, and the lipid complexes were incubated at 37 °C for 20 min in the dark. The lipid complexes were directly added to each well containing MCF-7 cells and mixed gently by rocking. The cells were incubated at 37 °C in the presence of 5% CO_2. After 1 h, the medium was removed, and the cells were then washed 10 times with PBS. Fluorescence microscopy was carried using an OLYMPUS IX-71. The excitation light was attenuated with a neutral density filter and reflected to the cells with a dichroic mirror (488 nm) during the emission of fluorescence (>500 nm).

RESULTS

We previously investigated the stability of a DNA triplex in acidic conditions, suggesting that a parallel duplex formed with Hoogsteen base pairs such as G × C^+ and A × T (Figure 1) was as stable as an antiparallel duplex formed with Watson−Crick base pairs (*20*). Because the stability of the parallel-duplex critically depends on the pH, this led to the idea that a DNA sequence that can form both antiparallel- and parallel-stranded duplexes would transition from the antiparallel-stranded duplex to the parallel-stranded duplex as the pH decreases (*20*). For this reason, we designed the parallel-stranded duplex of PyH1 (5′-TCTTTCTCTTCT-3′)·PuC1 (5′-AGAAAGAGAAGA-3′) to include fully matched base pairs in the parallel-stranded duplex, whereas at high pH, the antiparallel duplex PyH1·PuC1 would form a duplex with two bulges (Figure 1).

We first determined whether PyH1 (5′-TCTTTCTCTTCT-3′) and PuC1 (5′-AGAAAGAGAAGA-3′) form a pH-dependent parallel-stranded duplex. We examined the structure of the duplex at various pH values by CD (Figure 2). Our previous studies of a triple helix showed that a negative peak near 218 nm is induced by the parallel-stranded duplex containing Hoogsteen base pairs (*21*). We observed negative peaks at 218 nm in the present CD spectra of 70 μL of duplex in 100 mM Na^+ at pH 5.0, PyH1·PuC1. This negative CD intensity near 218 nm became more intense with increasing pH. Eventually, the peak near 218 nm became a positive peak, which is identical to that found with the antiparallel duplex. MD stimulation studies indicated that the parallel-stranded duplex (Hoogsteen form) is similar to that of a duplex with Hoogsteen base pairs in a DNA triple helix (*22*). Moreover, the UV mixing curve of PyH1 and PuC1 at pH 5.0 showed two straight lines intersecting at 50% PuC1, demonstrating formation of a 1:1 parallel complex (see the Supporting Information). Thus, the intensity change at 218 nm from low to high pH is due to a structural transition from a duplex with parallel strands to one with antiparallel strands.

We next examined the structure of the duplex at various pH values by UV melting measurements. Figure 3 shows the dependence of T_m on the pH in the presence of 100 mM NaCl and 4 μM total DNA. The T_m at pH 5.0, 6.0, and 7.0 was 30.0, 20.0, and 10.0 °C, respectively. Although the T_m at pH 5.0 was 10.0 °C higher than at pH 6.0 and 20.0 °C higher than at pH 7.0, the T_m values at pH 7.0, 8.0, and 9.0 were almost identical. Moreover, the free-energy values ($\Delta G°_{37}$) from single strand to parallel strand at pH 5.0, 5.5, and 6.0 were −8.0, −7.4, and −6.0 kcal/mol, respectively. Because the pH-dependent T_m and $\Delta G°_{37}$ are due to the protonation of a C base, the data indicate that the duplex is parallel-stranded at low pH.

Although BCECF and GFP are commonly used for monitoring the pH in living cells, they produce only a single

[1] Abbreviations: CD, circular dichroism; UV, ultraviolet spectroscopy; FITC, fluorescein isothiocyanate; TAMRA, tetramethylrhodamine.

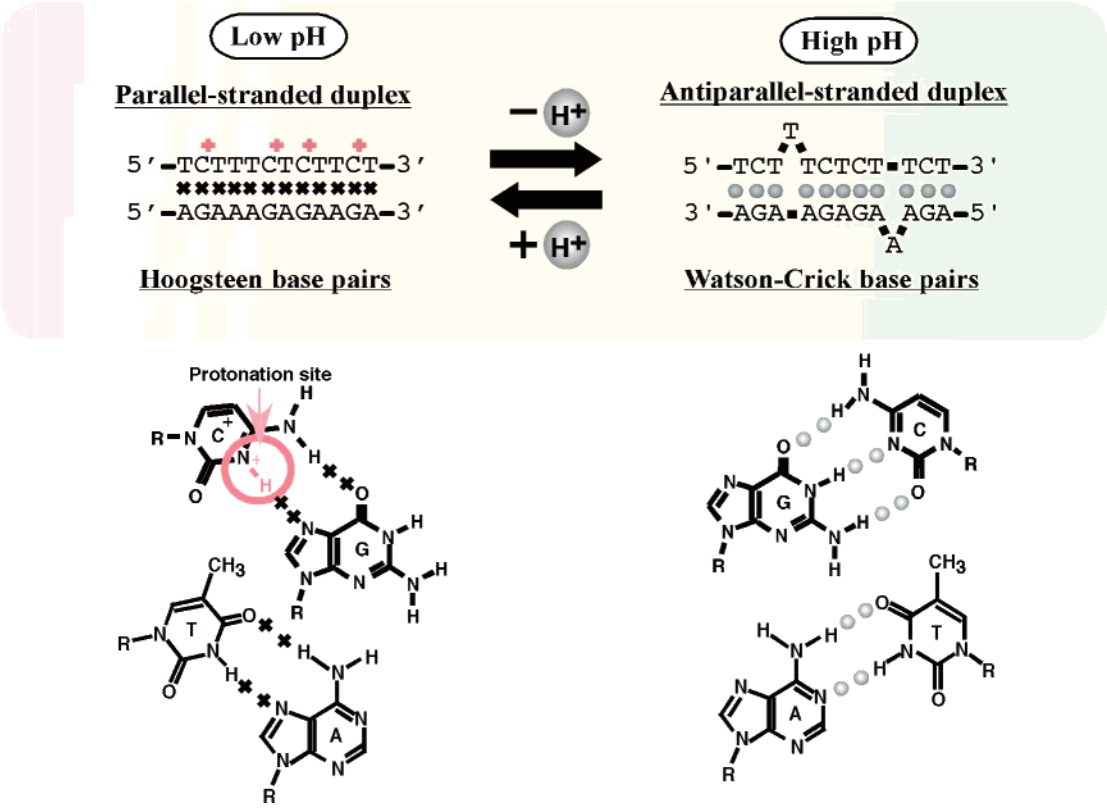

FIGURE 1: Structural transition between the antiparallel and parallel duplexes induced by pH change. The chemical structures of Hoogsteen base pairs A−T and G−C$^+$ of DNA parallel-stranded duplexes are shown.

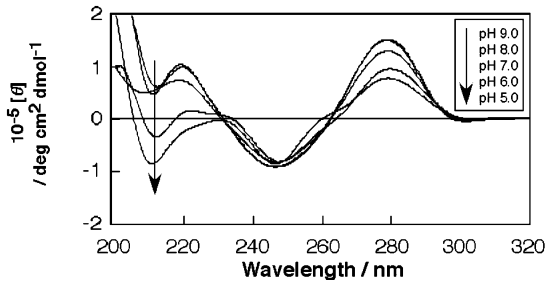

FIGURE 2: CD spectra of (5′-AGAAAGAGAAGA-3′/5′-TCTTTCTCTTCT-3′) in (a) 100 mM Na^+ and 50 mM Tris-acetate buffer (pH 5.0), 50 mM MES buffer (pH 6.0 or 7.0), or 50 mM Tris-HCl buffer (pH 8.0 or 9.0) at 1 °C. The spectra were obtained in the total DNA concentration of 70 μM.

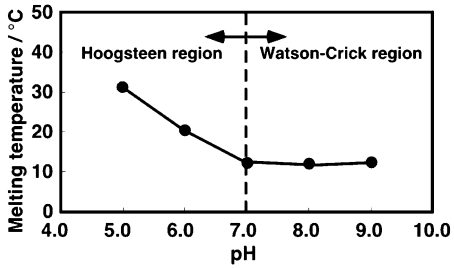

FIGURE 3: Dependence of the melting temperature on pH. Melting temperatures were calculated at approximately 4 μM of the total strand and in the presence of 100 mM Na^+ at various pH values.

color. Recently, fluorescent methods, such as FRET, have been developed for sensor molecules. FRET produces an easily detectable color change similar to that in molecular beacons (*9*). We therefore investigated whether FRET could be used in conjunction with the formation of a parallel-stranded DNA duplex to produce a detectable signal at low pH. Most FRET studies of nucleic acids have been carried out using FITC (excitation at 494 nm and emission at 525 nm) as the donor and TAMRA (excitation at 565 nm and emission at 580 nm) as the acceptor (*23*, *24*). For this reason, we covalently attached the 5′ ends of PyH1 and PuC1 to the donor (FITC) and acceptor (TAMRA) fluorophores, respectively. In this system, the efficiency of FRET should increase when the parallel-stranded duplex is formed and decrease when the antiparallel duplex is formed (Figure 4a). In this way, we reasoned that the fluorescently labeled DNA duplex would act as a pH-sensitive probe.

By measuring fluorescence emission, we followed the structural transition in the labeled PyH1·PuC1 duplex. Because the T_m value of 4 μM parallel duplex was 34 °C, we did not select 37 °C for measuring the fluorescence emission. When 4 μM duplex was excited at 494 nm in a buffer of 100 mM NaCl, 1 mM Na_2EDTA, and 50 mM Tris-HCl at pH 9.0 and 1 °C, we observed one positive peak near 517 nm, which corresponds with FITC emission (Figure 4a). In contrast, two peaks were observed near 517 and 570 nm at pH 5.0, corresponding to the FITC and TAMRA emissions, respectively (Figure 4a). Moreover, the intensity at 570 nm for the PyH1·PuC1 duplex with FITC and TAMRA was higher than that for the PyH1·PuC1 duplex with only TAMRA. Changes in pH did not affect the fluorescence of FITC- or TAMRA-labeled single strands or of mixed FITC- and TAMRA-labeled noncomplimentary oligonucleotides (data not shown). Together, these results indicate that FRET from FITC to TAMRA occurs only in the PyH1·PuC1 duplex under acidic conditions.

We next tested a system for directly visualizing the pH-dependent structural transition between the antiparallel- and parallel-stranded duplex. Figure 4b shows fluorescence

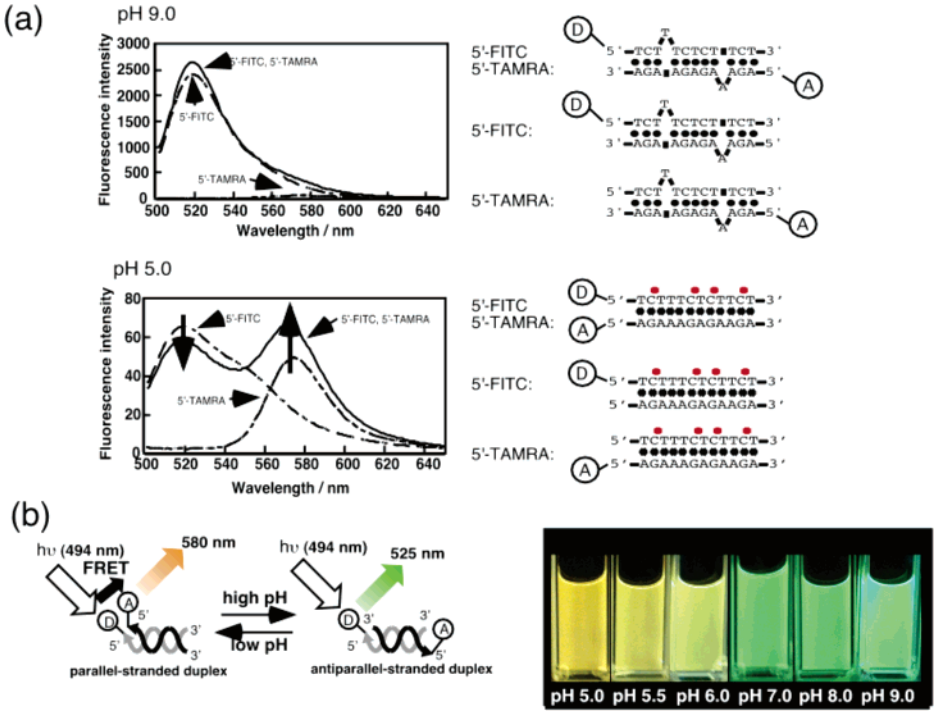

FIGURE 4: FRET measurements of parallel duplexes. (a) Fluorescence spectra of the DNA duplexes with excitation at 494 nm in the presence of 100 mM Na^+ and 1 mM Na_2EDTA at 1 °C and pH 9.0 or 5.0. (b) Photograph of fluorescence images of 4 μM DNA duplex (5′-FITC-TCTTTCTCTTCT-3′/5′-TAMRA-AGAAAGAGAAGA-3′) in the presence of 100 mM NaCl and 1 mM Na_2EDTA at various pH values.

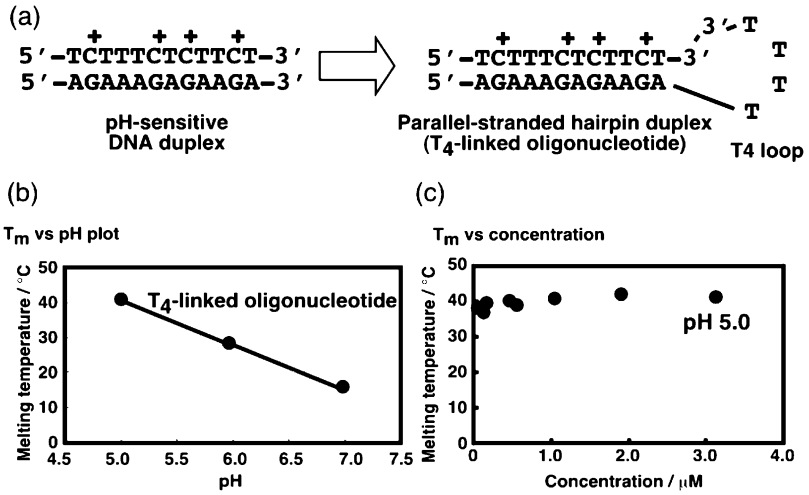

FIGURE 5: T_4-linked intramolecular parallel-stranded oligonucleotide. (a) Structures of the intermolecular parallel-stranded duplex and the T_4-linked intramolecular parallel-stranded oligonucleotide. (b) Dependence of the melting temperature on the pH. All melting temperatures were measured at approximately 3 μM of the total strand and in the presence of 100 mM Na^+ at various pH values. (c) Dependence of the melting temperature on the concentration of intermolecular parallel-stranded duplex. All melting temperatures were measured in the presence of 100 mM Na^+ at various pH values.

images of 4 μM duplex at various pH values excited by broad UV light with a λ_{max} at 360 nm. Green fluorescence (FITC) was observed at pH 9.0, while yellow fluorescence (TAMRA) was markedly intensified by the donor (FITC) at pH 5.0. These data show that the combination of FRET and the pH-sensitive DNA duplex is promising for the development of an easily visualized pH sensor.

Although the pH-sensitive intermolecular parallel-stranded duplex is easily applied to measuring pH in solution, measuring pH in living cells is more difficult because the net concentrations of the two oligonucleotides in living cells are very low, which decreases the T_m for parallel-stranded duplexes (*25*). We therefore designed an oligonucleotide that should form an intramolecular parallel-stranded duplex connected by a hairpin structure to provide thermodynamic stability independent of its concentration (*25*). This oligonucleotide was made by conjugating the 3′ ends of PyH1 and PuC1 with a sequence of four T bases (Figure 5a). As expected for such a structure, the T_m of this T_4-linked oligonucleotide was dependent on the pH under acidic conditions (i.e., pH 5.0−7.0) (Figure 5b) and, at pH 5.0, independent of the DNA concentration (Figure 5c). At pH 9.0, the UV melting curve for the intramolecular parallel-stranded duplex had a broad shape (see the Supporting Information), suggesting that the parallel hairpin is unstable at this pH. Thus, the data indicate that the T_4-linked

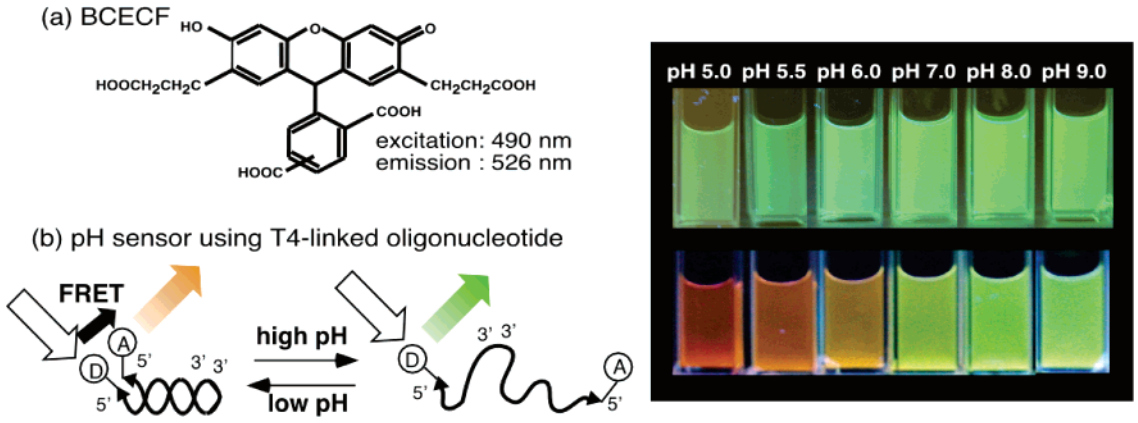

FIGURE 6: Photograph of T_4-linked oligonucleotide sensor *in vitro*. (a) Photograph of the fluorescence of BCECF at various pH values. (b) Photograph of the increased emission of acceptor (TAMRA) in the presence of the T_4-linked oligonucleotide sensor (5′-FITC-TCTTTCTCTTCT-3′/3′-TTTTAGAAGAGAAAGA-TAMRA-5′). All measurements were conducted in 100 mM NaCl and 1 mM Na_2-EDTA at various pH values.

oligonucleotide forms a hairpin parallel-stranded duplex at low pH.

We next investigated whether, like the intermolecular parallel-stranded duplex, the T_4-linked oligonucleotide could be labeled with fluorophores and used as a pH-sensitive probe. Figure 6 shows fluorescence images of 4 μM T_4-linked duplex at various pH values when excited by broad UV light with λ_{max} at 360 nm. Green fluorescence (FITC) was observed at pH 9.0, and orange fluorescence (TAMRA) was significantly intensified by the donor (FITC) at pH 5.0. Also, TAMRA-conjugated control DNA did not show clear orange fluorescence (see the Supporting Information). In addition, the orange fluorescence was clearer than with the unconjugated intermolecular DNA sensor. In contrast, the BCECF fluorescence changed only in intensity. Thus, in comparison to BCECF and the intermolecular complex (Figure 4b), the T_4-linked oligonucleotide is the most promising pH sensor because it has the widest dynamic color range.

Finally, we wanted to determine whether the T_4-linked intramolecular oligonucleotide could be coupled with fluorescence microscopy to assess pH changes in living cells. However, before cell imaging, it was necessary to examine its resistance to nucleases (see the Supporting Information). The intermolecular duplex and T_4-linked intramolecular oligonucleotide were incubated for 1 h at 37 °C with exonuclease or S1 nuclease. Although the intermolecular duplex was efficiently degraded by exonuclease or S1 nuclease, the T_4-linked intramolecular oligonucleotide was almost undegraded by either enzyme for at least 1 h. This is probably due to the 5′ modification of the T_4-linked intramolecular oligonucleotide (*26*).

To assess the utility of the T_4-linked intramolecular oligonucleotide for measuring pH changes in living cells, we used fluorescence microscopy to follow the color changes in MCF-7 human breast cancer cells undergoing [D-Trp^8]-SST peptide-induced apoptosis (*27*). Treatment with [D-Trp^8]-SST has been reported to cause a decrease in the intracellular pH from 7.25 to 6.45 in these cells (*27*). After incubation for 24 h with or without 100 nM [D-Trp^8]SST peptide, the MCF-7 cells were transfected for 1 h with 6 μM T_4-linked PyH1·PuC1 duplex using LipofectAMINE. Figure 7 shows that MCF-7 cells with or without [D-Trp^8]SST showed green (FITC) or orange (TAMRA) fluorescence, respectively. A T_4-linked oligonucleotide conjugated with only TAMRA did not show orange fluorescence (data not shown). In addition, we found that the peptide caused a 4-fold increase in the activities of caspases 3 and 7, which are cysteine aspartic-acid-specific proteases that participate in mammalian apoptosis (data not shown). Collectively, these results indicate that this novel DNA-based sensor coupled with FRET can detect pH changes in living cells.

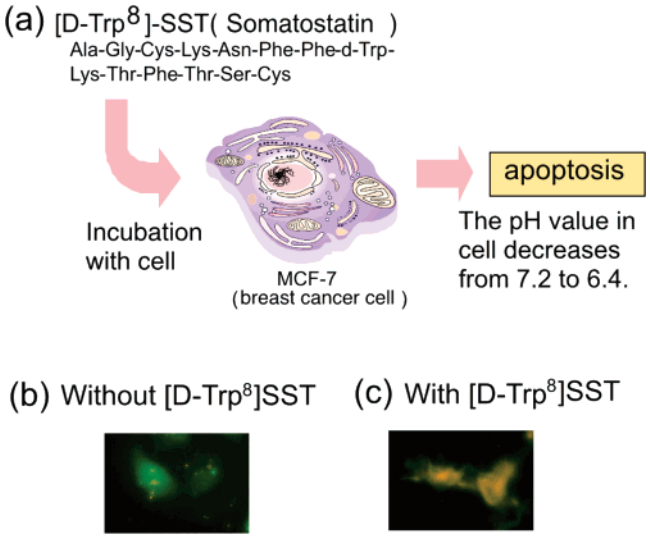

FIGURE 7: Photograph of T_4-linked oligonucleotide sensor in a living cell. Photograph of the fluorescence of the novel pH sensor in the absence of [D-Trp^8]-SST and in the presence of 100 nM [D-Trp^8]-SST. The excitation light was attenuated with a neutral density filter and reflected into the cells with a dichroic mirror (488 nm).

DISCUSSION

An ideal fluorescent pH sensor should have high sensitivity and a specific signal response to changes in pH. Our results show that the DNA indicator can measure intracellular pH with little background and no indicator leakage. The pH sensor drastically changes its color from green to orange as the pH decreases.

GFP has been used to determine pH in living cells because its absorbance and fluorescence are strongly pH-dependent in aqueous solutions and intracellular compartments of living cells (*28*). Titration of pH using purified recombinant GFP with a mutation reveals a >10-fold reversible change in its

absorbance and fluorescence and pK_a values of 6.0, 5.9, 6.1, and 4.8 (*28*). The pH sensitivity of GFP involves both protonation and conformational changes at lower pH, which are due to the mutation of the GFP. Although the pK_a values of GFP can be modified by further mutagenesis, it is hard to predict their pK_a values. In contrast, on the basis of the structure transition, the pK_a of our pH sensor was 6.7 (data not shown), suggesting that the DNA sensor is sensitive to pH values between 6.0 and 7.0, similar to the pH range in living cells. Moreover, because the pH dependence is due to the thermodynamic properties of the parallel-stranded duplex (unpublished observations), it should be possible to use thermodynamic calculations to predict the pK_a value of a duplex with modified sequences. Thus, the DNA-based pH indicator should be suitable for detecting pH changes in living cells. Furthermore, addition of ammonium chloride caused rapid changes in its color (unpublished data), demonstrating that it should be useful for continuous measurements of the pH in cells.

DNA also has the advantage that, compared to other materials used as biosensors, it can be easily used in living cells. Furthermore, many other organic biosensors need to be combined with an essentially irreversible enzyme-mediated modification to obtain a large spectral shift. Thus, in contrast to the DNA-based probe, other materials employed as probes cannot be used to analyze reversible reactions. In addition, given its reversibility, it may be possible to develop DNA-based probes for detecting other reversible reactions *in vitro* and in living cells.

In summary, we have described a new strategy for monitoring the intracellular pH that takes advantage of FRET and the transition in a DNA duplex from antiparallel- to parallel-strand orientation. We expect that this novel DNA-based pH sensor will be used as a probe for investigating biological processes in living cells.

SUPPORTING INFORMATION AVAILABLE

UV mixing curve of PyH1·PuC1, UV melting curve of T_4-linked intramolecular oligonucleotide, photograph of fluorescence of TAMRA-conjugated control DNA, and PAGE showing nuclease resistance of the intramolecular DNA oligonucleotides. This material is available free of charge via the Internet at http://pubs.acs.org.

REFERENCES

1. Potyrailo, R. A., Conrad R. C., Ellington A. D., and Hieftje G. M. (1998) Adapting selected nucleic acid ligands (aptamers) to biosensors, *Anal. Chem. 70*, 3419−3425.
2. Jhaveri, S., Rajendran, M., and Ellington, A. D. (2000) *In vitro* selection of signaling aptamers, *Nat. Biotechnol. 18*, 1293−1297.
3. Silverman, S. K. (2003) Rube Goldberg goes (ribo)nuclear? Molecular switches and sensors made from RNA, *RNA 9*, 377−383.
4. Ohmichi, T., Nakamuta, N., Yasuda, K., and Sugimoto, N. (2000) Kinetic property of bulged helix formation: Analysis of kinetic behavior using nearest-neighbor parameters, *J. Am. Chem. Soc. 122*, 11286−11294.
5. Sugimoto, N., Satoh, N., Yasuda, K. and Nakano, S. (2001) Stabilization factors affecting duplex formation of peptide nucleic acid with DNA, *Biochemistry 40*, 8444−8451.
6. Ohmichi, T., Nakano, S., Miyoshi, D., and Sugimoto, N. (2002) Long RNA dangling end has large energetic contribution to duplex stability, *J. Am. Chem. Soc. 124*, 10367−10372.
7. Miyoshi, D., Nakao, A, and Sugimoto, N. (2002) Molecular crowding regulates the structural switch of the DNA G-quadruplex, *Biochemistry 41*, 15017−15024.
8. Nakano, S., Uotani, Y., Nakashima, S., Anno, Y., Fujii, M., and Sugimoto, N. (2003) Large stabilization of a DNA duplex by the deoxyadenosine derivatives tethering an aromatic hydrocarbon group, *J. Am. Chem. Soc. 125*, 8086−8087.
9. Li, W., Miyoshi, D., Nakano, S., and Sugimoto, N. (2003) Structural competition involving G-quadruplex DNA and its complement, *Biochemistry 42*, 11736−11744.
10. Okumoto, Y., Tanabe, Y., and Sugimoto, N. (2003) Immobilized small deoxyribozyme to distinguish RNA secondary structures, *Biochemistry 42*, 2158−2165.
11. Okumoto, Y., Ohmichi, T., and Sugimoto, N. (2002) Factors that contribute to efficient catalytic activity of a small Ca^{2+}-dependent deoxyribozyme in relation to its RNA cleavage function, *Biochemistry 41*, 2769−2773.
12. Coskun, T., Chu, S., and Montrose, M. H. (2001) Intragastric pH regulates conversion from net acid to net alkaline secretion by the rat stomac, *Am. J. Physiol. 281*, G870−G877.
13. Grinstein, S., and Furuya, W. (1984) Amiloride-sensitive Na^+/H^+ exchange in human neutrophils: Mechanism of activation by chemotactic factors, *Biochem. Biophys. Res. Commun. 122*, 755−762.
14. Moolenaar, W. H., Tertoolen, L. G. J., and de Laat, S. W. (1984) Phorbol ester and diacylglycerol mimic growth factors in raising cytoplasmic pH, *Nature 312*, 371−374.
15. Pouyssegur, J., Sardet, C., Franchi, A., L'Allemain, G., and Paris S. (1984) A specific mutation abolishing Na^+/H^+ antiport activity in hamster fibroblasts precludes growth at neutral and acidic pH, *Proc. Natl. Acad. Sci. U.S.A. 81*, 4833−4839.
16. Matsuyama, S., Llopis, J., Deveraux, Q. L., Tsien, R. Y., and Reed, J. C. (2000) Changes in intramitochondrial and cytosolic pH: Early events that modulate caspase activation during apoptosis, *Nat. Cell Biol. 2*, 318−325.
17. Chacon, E., Reece, J. M., Nieminen, A. L., Zahrebelski, G., Herman, B., and Lemasters, J. J. (1994) Distribution of electrical potential, pH, free Ca^{2+}, and volume inside cultured adult rabbit cardiac myocytes during chemical hypoxia: A multiparameter digitized confocal microscopic study, *Biophys. J. 66*, 942−952.
18. Llopis, J., McCaffery, J. M., Miyawaki, A., Farquhar, M. G., and Tsien, R. Y. (1998) Measurement of cytosolic, mitochondrial, and Golgi pH in single living cells with green fluorescent proteins, *Proc. Natl. Acad. Sci. U.S.A. 95*, 6803−6808.
19. Pérez-Sala, D., Collado-Escobar, D., and Mollinedo, F. (1995) Intracellular alkalinization suppresses lovastatin-induced apoptosis in HL-60 cells through the inactivation of a pH-dependent endonuclease, *J. Mol. Biol. 270*, 6235−6242.
20. Sugimoto, N., Wu, P., Hara, H., and Kawamoto, Y. (2001) pH and cation effects on the properties of parallel pyrimidine motif DNA triplexes, *Biochemistry 40*, 9396−9405.
21. Wu, P., Kawamoto, Y., Hara, H., and Sugimoto, N. (2002) Effect of divalent cations and cytosine protonation on thermodynamic properties of intermolecular DNA double and triple helices, *J. Inorg. Biochem. 91*, 277−285.
22. Osborne, S. E., Cain, R. J., and Glick, G. D. (1997) Structure and dynamics of disulfide cross-linked DNA triple helices, *J. Am. Chem. Soc. 119*, 1171−1182.
23. Stojanovic, M. N., de Prada, P., and Landry, D. W. (2001) Aptamer-based folding fluorescent sensor for cocaine, *J. Am. Chem. Soc. 123*, 4928−4931.
24. Kuhn, H., Demidov, V. V., Coull, J. M., Fiandaca, M. J., Gildea, B. D., and Frank-Kamenetskii, M. D. (2002) Hybridization of DNA and PNA molecular beacons to single-stranded and double-stranded DNA targets, *J. Am. Chem. Soc. 124*, 1097−1103.
25. Rentzeperis, D., Kharakoz, D. P., and Marky, L. A. (1991) Coupling of sequential transitions in a DNA double hairpin: Energetics, ion binding, and hydration, *Biochemistry 30*, 6276−6283.
26. Warashina M., Kuwabara T., Nakamatsu Y., and Taira K. (1999) Extremely high and specific activity of DNA enzymes in cells with a Philadelphia chromosome, *Chem. Biol. 6*, 237−250.
27. Thangaraju, M., Kamal Sharma, K., Liu, D., Shen, Shi-H., and Srikant, C. B. (1999) Interdependent regulation of intracellular acidification and SHP-1 in apoptosis, *Cancer Res. 50*, 1648−1654.
28. Kneen, M., Farinas, J., Li, Y, and Verkman, A. S. (1998) Green fluorescent protein as a noninvasive intracellular pH indicator, *Biophys. J. 74*, 1591−1599.

BI0476782